JOURNAL OF CATALYSIS **164,** 122–130 (1996)
ARTICLE NO. 0368

CO_2-Reforming of Methane on Supported Rh and Ir Catalysts

Michael F. Mark and Wilhelm F. Maier[1]

Max-Planck-Institut für Kohlenforschung, Kaiser-Wilhelm-Platz 1, D-45470 Mülheim, Germany

Received March 24, 1995; revised September 26, 1995; accepted July 29, 1996

The effect of catalyst structure on CO_2 reforming of methane has been studied in the temperature range 550–850°C with oxide-supported Rh and Ir catalysts under conditions of reaction rate control. It is found that the rate of reaction expressed per unit metal surface area is constant over a wide dispersion range. There is no detectable effect of the pore structure or nature of the support on the reaction rate. By variation of feed composition through addition of steam or oxygen the H_2/CO ratio in the product could be varied.

INTRODUCTION

In recent years the utilization of the "greenhouse" gases carbon dioxide and methane has received increasing attention (1–3). The catalytic reforming of methane with CO_2, the so-called CO_2 reforming (1), is a particularly elegant way to combine CH_4 and CO_2 utilization (4–6). Our interest in this reaction was generated by the possible use of waste gases, e.g., biogas (agriculture, waste water treatment facilities) and flue gas (power plants), as sources for methane and CO_2.

$$CH_4 + CO_2 \rightleftharpoons 2\,CO + 2\,H_2 \qquad \Delta H_f^\circ = 247\ \text{kJ mol}^{-1} \quad [1]$$

The reaction product ("syngas") is a valuable feedstock for the production of higher hydrocarbons (Fischer–Tropsch synthesis) or methanol and for carbonylation processes (3). CO_2 reforming of CH_4 is also used as a chemical energy storage and energy transmission system (CETS) (7, 8). Solar energy is used to drive the endothermic forward reaction, and the energy thus stored can be transported via pipelines as syngas and liberated at will by the reverse reaction at any location or time.

The main reaction is accompanied by several secondary processes (Eqs. [2]–[5]), of which the reverse water–gas shift reaction appears to be the most important because of its dependence on the product hydrogen of reaction [1] (4, 9, 10).

$$CO_2 + H_2 \rightleftharpoons CO + H_2O \qquad \text{reverse water–gas shift reaction} \quad [2]$$

$$CO_2 + 4\,H_2 \rightleftharpoons CH_4 + 2\,H_2O \qquad \text{methanation} \quad [3]$$

$$2\,CO \rightleftharpoons C + CO_2 \qquad \text{Boudouard reaction} \quad [4]$$

$$CH_4 \rightleftharpoons C + 2\,H_2 \qquad CH_4\ \text{cracking} \quad [5]$$

Depending on the reaction conditions and on the composition of the gas mixture, carbon build-up due to the Boudouard reaction and methane cracking becomes thermodynamically favorable (9) and must be avoided by kinetic control (i.e., by the use of catalysts which do not catalyze coking reactions) to ensure that reforming is free of coking (10). Erdöhelyi *et al.* noted that reproducible results were obtained only at stoichiometric composition or with excess of carbon dioxide (5). Bodrov and Apel'baum noted already in 1966 that carbon lay-down is the dominating reaction under conditions of methane excess in the feed and they recommended a CO_2/CH_4 ratio > 1 for the investigation of the reforming reaction (11). The facile decomposition of methane at reforming temperatures is well-known. Solymosi *et al.* noted the formation of three different carbon species, depending on temperatures and various noble metals (12). This was confirmed by Zhang and Verykios on Ni/alumina catalysts (13). While at 500°C coking from methane is very low, a drastic increase is observed at 650°C (4). Swaan *et al.* (14) attribute the origin of CO formation to the Bouduard reaction [4]; they also showed by ^{13}C labeling that the reactive surface carbon in CO_2 reforming originates from CH_4, while the less reactive carbon accumulation follows the catalyst deactivation rate. In contrast to Swaan *et al.*, based on another ^{13}C labeling experiment, Tsipouriari *et al.* claim that carbon species accumulated during the reforming reaction originate from CO_2 (15). However, considering the above reaction network these studies lack the necessary control experiments to provide better evidence for such controversial findings. Coking-free reforming of methane under conditions of methane excess in the feed is reported to occur with specially prepared Rh and Ir catalysts only (6). However, methane conversion in these experiments is kept below the CO_2 content in the feed, presumably since stoichiometry would enforce coking at higher methane conversions. Excess of CO_2 in the feed is known to result in an increase of CO formation and high methane conversions (6).

---

[1] To whom correspondence should be addressed.

0021-9517/96 $18.00

Conditions of CO_2 excess in the feed are being utilized in the commercial Calcor process for the production of clean CO (16).

Little is known about the catalyst structure activity relationship and the surface structure sensitivity of the reforming reaction, parameters which are important for catalyst optimization. Nakamura *et al.* (17) observed widely different turnover frequencies Rh which decreased in the order $Rh/TiO_2 > Rh/Al_2O_3 > Rh/SiO_2$, although too few data render the importance of this study hard to judge. Tsipouriari *et al.* report a significant dependence of the reforming reaction on Rh crystallite size and support with the following decreasing activity $YSZ > Al_2O_3 > TiO_2 > SiO_2 > MgO$ (15). Erdöhelyi *et al.* (18) did not find significantly different turnover frequencies on Rh catalysts based on Al_2O_3, TiO_2, SiO_2, or MgO. They have stated that, in sharp contrast to CO and CO_2 hydrogenation and the $NO + CO$ reaction, the methane reforming reaction at high temperatures on supported Rh catalysts depends hardly at all on the nature of the support (18), while with Pd-based catalysts the observed activity decreases in the following order: $TiO_2 > Al_2O_3 > SiO_2 > MgO$ (5).

Thermodynamic equilibrium calculations (10) on the temperature dependence of the composition of a 1 : 1 starting mixture of CH_4 and CO_2 show that a conversion of 50% and a water content maximum of about 10% are obtained at around 600°C. Due to the above side reactions, the H_2/CO ratio in the temperature range 400–800°C is always significantly below 1. A CH_4 equilibrium conversion of >90% requires reaction temperatures above 750°C; here the H_2/CO product ratio is already 0.9. The desired H_2/CO ratio of 1 is only reached at temperatures above 1000°C. In these calculations carbon deposition was explicitly excluded.

The reaction mechanism of CO_2 reforming is still in doubt. Erdöhelyi *et al.* (5) and Rostrup-Nielsen and Bak-Hansen (4) propose a mechanism based on the dissociative adsorption of CH_4 and CO_2 followed by the rate determining surface reaction of the adsorbed dissociation products. CH_4 dissociation is assumed to form partly dehydrogenated CH_x species and surface C species, while CO_2 dissociates to CO and O.

$$CH_4 + z \rightarrow CH_x\text{-}z + (4 - x)/2\ H_2 \rightarrow C\text{-}z + 2\ H_2 \quad [6]$$

$$CO_2 + 2\ z \rightarrow CO\text{-}z + O\text{-}z \quad [7]$$

$$O\text{-}z + C\text{-}z \rightarrow CO\text{-}z \quad [8]$$

$$CO\text{-}z \rightarrow CO + z \quad [9]$$

z indicates a surface site. The CO_2 dissociation is believed to be enhanced by codissociation of CH_4 to CH_x-z species.

We have shown that the mechanism of the reaction between CH_4 and CO_2 on Rh/Al_2O_3 catalysts under normal pressure at 700°C is more adequately described by a stepwise process (19). In a slow rate-determining first step, active carbon and free hydrogen are generated by the dissociative adsorption of CH_4 on active metal sites. In the faster second step, the active carbon reacts with CO_2 to form two equivalents of CO.

$$CH_4 + z \rightarrow C_{ads} + 2\ H_2 \quad \text{rate determining step} \quad [10]$$

$$C_{ads} + CO_2 \rightarrow 2\ CO \quad \text{fast} \quad [11]$$

This reaction mechanism was also confirmed on Ru and Ir/Al_2O_3 catalysts (20).

Besides high initial activity, the long term stability under the drastic reaction conditions required for high CH_4 conversions has to be considered. For technical applications the conditions and limits for variation of the H_2/CO product ratio are of fundamental importance. Thermodynamic equilibrium calculations show that partial replacement of CO_2 by H_2O or O_2 results in an increase in the H_2/CO ratio of the equilibrium gas mixture. The close relationship between the CO_2 reforming reaction and the steam reforming of methane has already been documented (4, 7). Hence the reaction behavior of methane with mixtures of CO_2, H_2O, and O_2 under reforming conditions may allow excellent control over syngas composition.

A detailed kinetic study was conducted in conjunction with the present work (21). The study covered the wide temperature range 500–850°C. Kinetic modeling of the CO_2 reforming of a 1 : 1 (CH_4/CO_2) mixture on an Ir/Al_2O_3 catalyst was carried out by numerical integration of selected rate equations and direct fitting to the experimental data over the whole temperature range. It was found that the experimental data could be reproduced by several kinetic models, but the best fit and the only one to provide meaningful parameters over the whole temperature range studied was obtained with the following rate equation, derived from the proposed stepwise mechanism:

$$r_{\text{Ref}} = \frac{k_{\text{Ref}}\left(p_{CH_4} - \left(p_{H_2}^2 p_{CO}^2 / K_{\text{Ref}} p_{CO_2}\right)\right)}{1 + \left(p_{CO}^2 / K_{\text{R,C-}z} p_{CO_2}\right)} \quad [12]$$

This kinetic study also confirms that under the reaction conditions reported below, the chemical reaction is rate determining and is not affected by transport phenomena.

EXPERIMENTAL

Catalysts

All catalysts were prepared by conventional wet impregnation techniques. Besides commercially available Al_2O_3 and TiO_2, various catalyst supports were prepared via the sol–gel process (22). The preparation of sol–gel Al_2O_3, SiO_2, and ZrO_2 has been described in detail (23). Binary oxides containing SiO_2 as the main component were prepared by mixing the appropriate amounts of $Si(OC_2H_5)_4$ with $Zr(n\text{-}OC_3H_7)_4$, $Ti(i\text{-}OC_3H_7)_4$, or $Al(sec\text{-}OC_4H_9)_3$, diluting with ethanol (99%) and introducing HCl (8 *M*) to catalyze the gelling process. Prior to impregnation all support materials were first dried at room temperature, heated to 65°C for 5 h, and finally heated to 250°C for 4 h with a heating rate of $0.2^\circ\ \mathrm{min}^{-1}$. The metal precursors ($RhCl_3 \cdot 3\ H_2O$, $IrCl_3 \cdot 3\ H_2O$, $RuCl_3$, $Pd(NO_3)_2$ and H_2PtCl_6) were dissolved in about 10 ml of aqueous HCl (0.8 *M*). About 2 g of the freshly calcined support was added to the solution and this slurry was stirred for 24 h at room temperature and then dried at 393 K for 24 h. All catalyst particles were milled and sieved; the sieve fraction 50–200 μm was used for the activity study. Light microscopy investigation of this sieve fraction showed all particles $> 50\ \mu$m.

In some cases a different approach was used: the precious metal precursor was added during the gelling process to fix the precursor compound in the sol–gel matrix.

Characterization of the Catalysts

The support surface area (BET) and pore structure (Dollimore–Heal) were determined from the N_2 adsorption isotherms at 77 K. For purely microporous materials the surface area was calculated by the method of Dubinin and the pore size distribution by the procedure of Horvath–Kawazoe. Metal dispersions were measured by the CO pulse chemisorption method at room temperature. An adsorption stoichiometry of $CO : M_s = 1$ was assumed, although CO adsorption on precious metals occurs in linear and bridged form and therefore the assumed adsorption stoichiometry is only an approximation. The same applies to the assumed adsorption stoichiometry of $1/2\ O_2 : Me = 1$ (see below), since oxygen adsorption may lead to partial bulk oxidation of metal crystallites. All catalysts were prereduced at 600°C for 2 h in flowing hydrogen before chemisorption measurements. The metal dispersion of catalysts based on supports containing Zr or Ti could not be determined by CO chemisorption due to a nearly total suppression of CO adsorption after prereduction at 600°C. After reduction at 300°C a significant CO uptake could be detected. A likely explanation for the suppressed CO adsorption after reduction at high temperature is the SMSI effect (24) (SMSI: Strong-Metal-Support-Interaction). Oxygen pulse chemisorption is recommended for supported noble metal catalysts with SMSI behavior (24–26). An adsorption stoichiometry of $1/2\ O_2 : M_s = 1$ was used to determine the dispersion of these catalysts (24, 25). A significant amount of O_2 adsorption on the pure carrier was detected. O_2 adsorption on prereduced titania and zirconia is well-known. We found that the amount adsorbed after standard prereduction procedure is well-reproducible. To determine the amount of O_2 chemisorbed on the precious metal the O_2 amount adsorbed on the pure carrier was subtracted from the total O_2 amount adsorbed on the examined catalyst. Cross checks on the dispersion gave identical values within the experimental error (1% Rh/Al_2O_3 sample: $D_{CO} = 22 \pm 2$, $D_{O_2} = 25 \pm 4$). TEM micrographs on the 1% $Rh/ZrO_2\ SiO_2$ ($D_{O_2} = 25\%$ corresponding to crystallites of about 4–5 nm) showed Rh crystallites in the range 2–7 nm and on the 0.5% Rh/Al_2O_3 catalyst ($D_{CO} = 33\% \sim$ 3–4 nm) crystallites in the size range 3–10 nm were detected. No statistical distribution of particle sizes from the TEM micrographs was obtained, since the error of this method is large for small crystallites, which are hard to recognize because of poor contrast. The described procedures for chemisorption have been selected after careful checking for reproducibility and reliability. Although the absolute numbers of the reported dispersions may be in error, the error will be a systematic one, not affecting the relative changes of accessible metal surface area.

Activity Tests

Activity tests were carried out in a conventional flow system at atmospheric pressure with a tubular fixed bet quartz reactor (inner diameter 8 mm). A thermocouple was placed in the catalyst bed to monitor the reaction temperature. The reaction gases were of the commercial purity H_2 (quality 5.0), O_2 (4.0), CH_4 (3.5), and CO_2 (3.5) and were dosed via mass flow controllers. An additional syringe pump was used for water addition. The products were analyzed by on-line gas chromatography (packed column Haye Sep A 17′, carrier gas Ar, WLD 120°C, temperature program: 3 min at 35°C, heating rate 30°C/min to 80°C). Catalyst loadings of 30 mg were diluted with 120 mg $\alpha\text{-}Al_2O_3$ and held in position in the reactor by quartz wool. The following experimental conditions were used for a typical run: The catalyst was reduced *in situ* at 600°C for 2 h in flowing hydrogen (20 ml min^{-1}). The gas flow was switched to a 1 : 1 (CH_4/CO_2) gas mixture (35 ml min^{-1}). The reaction was monitored for 2–3 h at high temperature (ca. 850°C) until steady state conditions were reached. GC samples were taken while consecutively lowering the reaction temperature until no more CH_4 conversion could be detected. CH_4 conversions were precise within an error of ±2% (absolute error). Consequently, low CH_4 conversions contain high experimental errors. Turnover frequencies (TOF, rates per unit surface area) were always determined under differential conditions (i.e., CH_4 conversions lower than 15%), since they should represent rates. The TOFs were calculated according to

$$\mathrm{TOF}_i = \frac{dX_i}{d(n_{Me,\mathrm{s}}/\dot{n}_{\mathrm{k,o}})} \overset{[X_i<10\text{–}20\%]}{\approx} \frac{X_i}{(n_{Me,\mathrm{s}}/\dot{n}_{\mathrm{k,o}})}, \qquad [13]$$

where TOF_i is the turnover frequency of component *i* [$\mathrm{mol}_i\ \mathrm{mol}_{Me,\mathrm{s}}^{-1}\ \mathrm{h}^{-1}$] and $n_{Me,\mathrm{s}}$ is the number of active surface sites [$\mathrm{mol\ g}^{-1}$].

RESULTS AND DISCUSSION

The study of catalyst structure activity relationships for the purpose of catalyst improvements requires that the reaction is first order in catalyst (no transport limitation, no gas phase reaction), that the catalyzed chemical reaction is rate determining, and that the same reaction step remains rate determining over the temperature range studied. A major concern in the investigation of heterogeneously catalyzed gas phase reactions is that of transport phenomena, which usually tend to become rate determining at higher temperatures. As the reforming reaction proceeds at high temperatures, reaction conditions have been carefully chosen to exclude such effects. Appropriate control experiments have been conducted, which showed that diffusional limitations can be excluded under our reaction conditions.

Choice of Feed Composition and Exclusion of Transport Limitations

The observation of uncontrollable coking of the catalysts under conditions of methane excess in the feed have initiated our mechanistic study (19). With increasing CO_2 in the feed, a decreasing H_2/CO ratio in the product (see Fig. 1) is indicative of a decreasing contribution of the reforming reaction [1] and an increasing contribution of the reverse water–gas shift (RWGS) reaction [2] to the overall process.

In all experiments where the reforming reaction itself was of primary interest, a stoichiometric feed composition of $CH_4 : CO_2 = 1$ was therefore applied.

Variation of the feed flow from 0.08 to 0.03 mol CH_4/h at a constant modified residence time τ_{mod} (variation of catalyst mass) on the 5% Rh/alumina and 1% Ir/alumina showed no effect on methane conversion excluding diffusional limitations (see Fig. 2). Only at flow rates significantly smaller than 0.03 mol/h can the onset of diffusional limitation be recognized. Table 1 shows that there is no effect of catalyst particle size on the methane conversion at 800°C, excluding pore diffusion limitation under these reaction conditions. These control experiments (27) confirmed the absence of transport and pore diffusion limitations under the conditions and catalysts reported here.

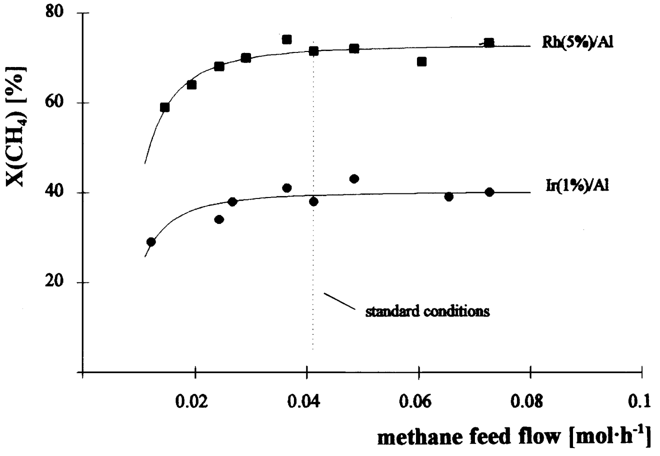

FIG. 1. Mass transport investigation. Dependence of methane conversion on feed at constant modified residence time, feed composition $CH_4/CO_2 = 1$.

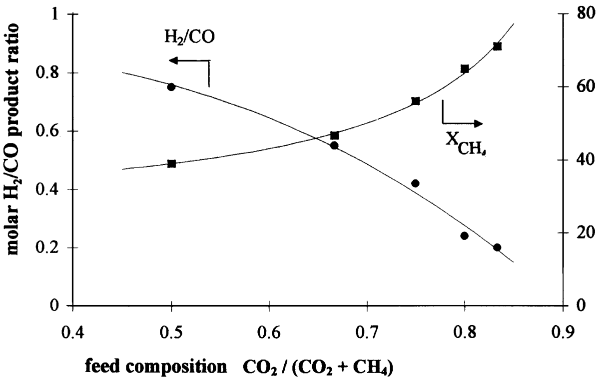

FIG. 2. Effect of CO_2 increase in the feed on product composition and CH_4 conversion at 750°C on 1% Rh/γ-Al_2O_3 at constant feed flow.

This surprising lack of transport limitations at such high reaction temperatures is attributed to the highly diluted catalyst bed, the small particle size of the catalyst, and the catalyst preparation, which consisted of direct impregnation of the small support particles.

Choice of Active Metal

To determine the catalytically most active metals, experiments with Rh, Ru, Ir, Pd, and Pt catalysts (metal content 0.5 wt%) supported on a commercially available γ-Al_2O_3 (Condea Pural 200) have been performed. Table 2 lists the results of the activity tests.

While Rh, Ir, and Ru catalysts showed stable long-term activity, Pd and Pt catalysts deactivated rapidly. The observed activity sequence of Rh > Ru > Ir ≫ Pd, Pt confirms earlier observations (4). On the Pd catalyst distinct coke

TABLE 1

Dependence of CH_4-Conversion on Catalyst Particle Sizes under Standard Reaction Conditions at 800°C (Diluted Catalyst Bed)

Catalyst	Particle size (μm)	CH_4 conversion X_{CH_4} (%)
Ir(1%)/γ-Al_2O_3	<20	37
	20–50	40
	50–200	38
	>200	41
Rh(1%)/ZrO_2 (5 mol%)/SiO_2	<20	66
	20–50	71
	50–200	68
	>200	67

TABLE 2

Comparison of Turnover Frequencies (Activities) of the Metal (0.5 wt%)/Al_2O_3-Catalysts for CO_2 Reforming of CH_4 under Standard Reaction Conditions

Metal	Precursor	Dispersion (%)	TOF (s^{-1})[a]
Rh	$RhCl_3 \cdot 3H_2O$	33 ± 5	4.0 ± 1.1
Ru	$RuCl_3$	35 ± 3	2.0 ± 0.6
Ir	$IrCl_3 \cdot 3H_2O$	22 ± 4	2.0 ± 1.3
Pd	Pd $(NO_3)_2$	15	<0.1
Pt	H_2PtCl_6	15	<0.1

[a] Turnover frequency (rate per unit metal surface area), measured at 700°C.

formation was observed. No other catalysts exhibited coking. This was confirmed by subsequent temperature programmed oxidation experiments (in flowing O_2, heating rate 20° min^{-1}) with the used catalysts: no CO_2 evolution could be detected on the Rh, Ru, Ir, and Pt catalysts.

Structure-Sensitivity Study

A potentially important parameter for catalyst design is the sensitivity of the reaction of interest to the surface structure, i.e., the crystal face of the active sites (28). Because of the change in surface composition for edge, kink, and terrace atoms with particle size, reactions which proceed with different rates (per unit metal surface area) over differently dispersed catalysts are termed *structure sensitive*; the rates of *structure insensitive* reactions are independent of the coordination at the active sites and proportional only to the total number of active sites present (29). Metal-catalyzed reactions with rates (expressed per unit surface area) sensitive to the metal particle size or metal dispersion are thus *structure sensitive* (30). To examine the influence of the metal dispersion on the catalyst activity, differently dispersed Rh and Ir catalysts supported on commercial γ-Al_2O_3 (Condea Pural 200) were prepared.

Two approaches were used to vary the metal dispersion. In one approach catalysts were prepared with different total metal loadings in the range from 0.5 to 5 wt%. With increasing metal content a decrease in metal dispersion is generally expected and was experimentally observed (exception: Ir catalyst with 0.5 and 1%, see Table 3). As previously reported for Pt (29) a convenient and reliable way to vary the metal dispersion was found to be the application of a tailored oxidation–reduction pretreatment to Rh and Ir catalysts of the same metal loading (metal content of 0.5 wt%), which reproducibly leads to catalysts with widely differing metal dispersions depending on the oxidation temperature. The support impregnated with the Rh or Ir salt was oxidized at temperatures varying between 300 and 800°C (30 min, flowing oxygen, 30 ml min^{-1}) leading to Rh or Ir oxide aggregates on the support surface. In a consecutive step the metal oxide is reduced at 600°C in flowing hydrogen. Preoxidation at 700°C produced the maximum dispersion for the Rh catalysts, whilst the maximum dispersion for Ir catalysts was reached by a milder oxidation pretreatment at 500°C (see Table 3). The observed enhancement of metal dispersion by a selected oxidation-reduction procedure is referred to in the literature as the redispersion effect (24). With the two approaches applied, Rh dispersions could be varied reproducibly in the range of 14 to 62% and Ir dispersions in the range of 8 to 49%.

Activity tests were performed with all catalysts. Results are listed in Table 3. All catalysts performed without observable deactivation. There was a strong correlation of the CH_4 conversion value with the accessible metal surface area, as shown in Fig. 3. An increase in metal surface area (i.e., in the number of active sites) leads to an increase in CH_4 conversion.

In Table 3 the high temperature activities of various catalysts are compared by the integral conversion of CH_4 at 750°C under steady state conditions. Since the equilibrium conversion at this temperature is 0.85, all data are still far from equilibrium and thus meaningful. From our kinetic study by comparison of the theoretical equilibrium constant K_{wgs} with the determined one, we know that at 600°C the water–gas shift reaction is about 50% and at 850°C about 10% away from equilibrium.

Due to the wide spread of conversions, a higher activity of the Rh catalysts relative to the Ir catalysts is the only reliable conclusion. To compare relative reaction rates, turnover frequencies determined under differential conditions

TABLE 3

Activities of Differently Dispersed Rh and Ir/Al_2O_3 Catalysts for CO_2 Reforming of Methane under Standard Reaction Conditions

Metal	Metal content (wt%)	T_{Ox} (°C)	D (%)	Metal surface area (m^2 g^{-1}cat)	X_{CH_4}[a] (%)	TOF (CH_4)[b] (s^{-1})
Rh	0.5	—	33 ± 5	0.75	36	1.2 ± 0.7
		300	38 ± 3	0.85	34	0.8 ± 0.5
		600	32 ± 4	0.73	31	1.2 ± 0.6
		700	62 ± 7	1.39	42	1.0 ± 0.4
		800	24	0.53	27	1.1 ± 0.8
	1	—	22 ± 2	0.98	39	1.1 ± 0.5
	2	—	18 ± 2	1.60	44	1.4 ± 0.4
	5	—	14 ± 1	3.14	49	1.0 ± 0.2
Ir	0.5	—	22 ± 4	0.26	11	2.2 ± 1.8
		300	44	0.53	17	2.6 ± 0.9
		500	49 ± 6	0.59	18	2.1 ± 0.8
		600	8	0.10	5	1.9 ± 4.0
	1	800	~0	~0	0	0
	1	—	45 ± 5	1.07	25	1.9 ± 0.5
	2	—	23 ± 4	1.10	23	1.7 ± 0.5
	5	—	15 ± 1	1.77	30	1.8 ± 0.4

[a] CH_4 conversion measured at 750°C ($X_{CH_4\text{–eq}} = 85\%$).

[b] TOF measured at 600°C (Rh) ($X_{CH_4\text{–eq}} = 41\%$) and 700°C (Ir) ($X_{CH_4\text{–eq}} = 73\%$), respectively.

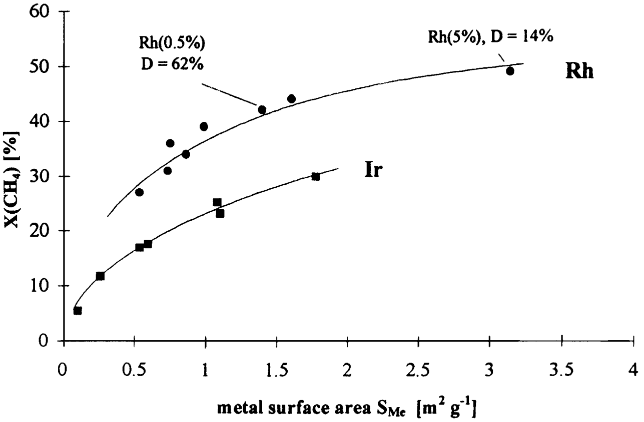

FIG. 3. Dependence of CH_4 conversion $X(CH_4)$ on the accessible metal surface area for various Rh and Ir/Al_2O_3 catalysts (reaction temperature 750°C).

(obtained at 600°C for Rh and 700°C for Ir) are shown in the last column. The reaction rates per unit surface area (TOF) show no trend and it must be concluded that the reaction is independent of the metal dispersion in the margin of experimental error. The results show that the CO_2 reforming of CH_4 can be classified as structure insensitive, indicating that the rate determining step of the reaction mechanism is independent of the particle size and thus of the surface structure of the active metal. Our earlier studies concerning the reaction mechanism (19) showed that the slow (rate determining) step is the generation of active carbon by the dissociation of methane on active sites. In view of our results presented here, this reaction step should be termed structure insensitive. This is in contrast to studies on single crystal surfaces, where methane activation has been found to be structure sensitive. However, at the high temperature of the reaction conditions in CO_2 reforming, surface reconstruction of the noble metal particles (a common and well-known effect at much lower temperatures in single crystal studies) may be so fast that the effect of certain surface structures would be cancelled.

A highly dispersed Rh catalyst with a low precious metal content should therefore be an economically effective catalyst combining high activity at relatively low cost. This is illustrated in Fig. 3: nearly identical CH_4 conversions are obtained with a highly dispersed Rh(0.5%) and a poorly dispersed Rh(5%) catalyst.

Influence of the Support on Catalyst Activity

To examine the influence of the support on the activity, various Rh(1%) catalysts were prepared. Besides commercial Al_2O_3 and TiO_2 supports, highly porous SiO_2, Al_2O_3, ZrO_2 and binary mixed oxides were prepared by the sol–gel method. The binary gels contain SiO_2 as a main component and 5 mol% of the oxide of a second metal (Al, Ti, and Zr). The sol–gel supports typically have higher surface areas and smaller pore diameters (mostly in the micropore range) than the commercial supports. Table 4 lists the physical properties of all the supports.

The activities of the Rh (1 wt%) catalysts based on these supports were determined under standard reaction conditions. All catalysts showed stable activity over the usual reaction time of 6–8 h. Table 5 lists the results of the experiments.

Figure 4, showing the dependence of CH_4 conversion on the accessible metal surface area on the various supports, illustrates a surprising independence of the conversion on the nature of the support. CH_4 conversion increases with increasing metal surface area, while the rate per unit surface area (TOF) calculated for the various catalysts remains constant within (considerable) experimental error. On the other hand, no correlation of catalyst activity with any physical properties of the supports could be detected. The activity depends only on the size of the accessible metal surface area. The influence of the support on the reaction is

TABLE 4

Physical Properties of the Supports

Support	Preparation or source	Modification[a]	Specific surface area ($m^2\ g^{-1}$)	Pore structure
α-Al_2O_3	calcined γ-Al_2O_3	α-Al_2O_3	~10	nonporous
γ-Al_2O_3	Condea Pural 200	γ-Al_2O_3	78	mesopores 40–70 nm
γ-Al_2O_3	Alfa Products	γ-Al_2O_3	150	mesopores ~40 nm
γ-Al_2O_3	sol–gel	ex-boehmite	190	meso- and micropores
ZrO_2	sol–gel	amorphous	240	micropores <1 nm
SiO_2	sol–gel	amorphous	840	micropores ~0.8 nm
ZrO_2(5%)/SiO_2	sol–gel	amorphous	610	micropores <1.5 nm
Al_2O_3(5%)/SiO_2	sol–gel	amorphous	510	meso- and micropores
TiO_2	Degussa	rutile	41	mesopores
TiO_2(5%)/SiO_2	sol–gel	amorphous	515	micropores <1 nm

[a] From X-ray powder diffraction analysis.

TABLE 5

Activities of Rh(1 wt%) Catalysts Based on the Supports Listed in Table 4

Support	D (%)	Metal surface area S_{Rh} ($m^2\,g^{-1}$)	$X_{CH_4}{}^b$ (%)	$TOF_{CH_4}{}^c$ (s^{-1})
α-Al_2O_3	16	0.71	32	1.5 ± 0.9
γ-Al_2O_3	22	0.98	39	1.1 ± 0.5
γ-Al_2O_3	28	1.24	53	1.1 ± 0.4
γ-Al_2O_3	26	1.16	45	0.6 ± 0.4
ZrO_2	16[a]	0.71	26	0.9 ± 0.7
SiO_2	8	0.36	16	1.2 ± 1.2
ZrO_2(5%)/SiO_2	25[a]	1.11	46	0.7 ± 0.5
Al_2O_3(5%)/SiO_2	5	0.22	14	2.0 ± 3.0
TiO_2	17[a]	0.76	35	1.3 ± 0.8
TiO_2(5%)/SiO_2	11[a]	0.49	29	1.2 ± 1.0

[a] Rh dispersion determined by O_2 chemisorption.

[b] CH_4 conversion measured at 750°C.

[c] TOF measured at 600°C.

therefore limited to affecting the metal dispersion during the course of the catalyst preparation and stabilizing the dispersion during catalyst use. These results underline the structure insensitivity of the CO_2 reforming even with different catalyst supports.

Long-term activity studies were performed with the most active catalysts (supports: ZrO_2(5%)/SiO_2 and γ-Al_2O_3 (Alfa Products)). No deactivation was observed after reaction times of 48 h at 750°C. To study the thermal stability further, both supports were heated to 700°C in air and their physical structure (i.e., surface area and porosity) was monitored with increasing calcination time: While the already lower surface area of 150 m^2/g of the commercial γ-Al_2O_3 was stable, the sol–gel derived ZrO_2(5%)/SiO_2 lost about 50% of its 610 m^2/g of surface area during the first 24 h. After this initial loss of surface area, both supports showed stable BET surface areas and pore structures even after more then 500 h at 700°C, confirming that both supports have a high thermal durability.

To prepare highly dispersed catalysts the direct introduction of the metal precursor compound during the sol–gel process was investigated. Besides saving the additional impregnation step, it was expected that the active metal would be immobilized in the sol–gel matrix ensuring homogeneously distributed metal sites especially resistant to sintering. Positive results were achieved by this catalyst preparation method for poison resistant hydrogenations of long chain hydrocarbons on membrane catalysts (31). Here, this preparation did not lead to improved catalyst performance. For example, a Rh/Al_2O_3 catalyst prepared by this method with a metal dispersion of 14% achieved a CH_4 conversion of 26% (at 750°C) compared to a dispersion of 26% and a CH_4 conversion of 46% for the conventionally prepared (impregnated) catalyst. We believe that the noble metal, when introduced directly into the glassy matrix via the sol–gel process, becomes partly inaccessible to the methane, while the hydrogen (see Ref. (25)) seems less affected due to its small size and spillover properties. In general, all catalysts prepared by direct introduction of the metal precursor during gelation showed significantly lower metal dispersions (presumably due to partial enclosure of the active sites by the sol–gel matrix) and consequently showed lower activity than catalysts prepared via the impregnation method.

Variation of the H_2/CO Ratio

By introducing H_2O or O_2 to the CH_4/CO_2 feed it was possible to increase the H_2/CO product ratio ($0.7 < H_2/CO < 3$), which confirmed thermodynamic calculations

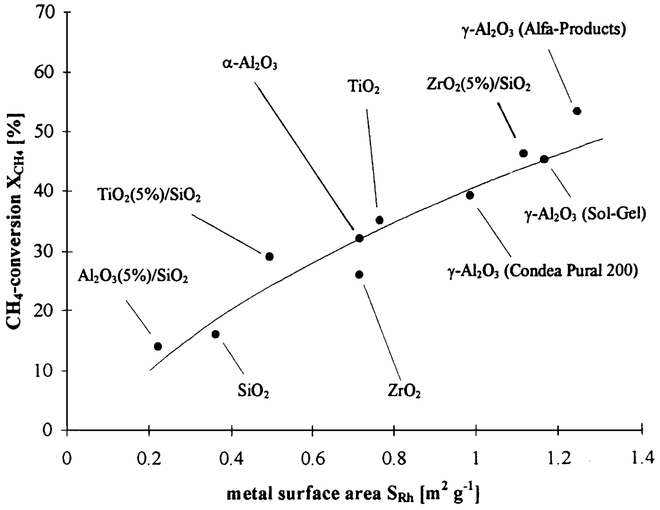

FIG. 4. Dependence of CH_4 conversion on the accessible metal-surface of Rh(1%) catalysts on various supports.

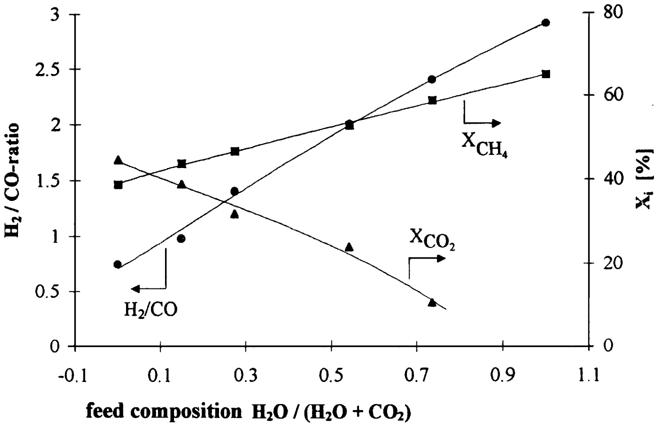

FIG. 5. Effect of steam addition to the feed on the product composition. Reaction temperature 750°C, 1% Rh/γ-Al_2O_3, feed $\dot{n}_{CO_2,0} + \dot{n}_{H_2O,0} = \dot{n}_{CH_4,0} = \text{const.}$).

on the equilibrium compositions of $CH_4/CO_2/H_2O$ or $CH_4/CO_2/O_2$ feed mixtures. The increase in H_2/CO ratio can be explained by the occurrence of additional CH_4 reforming reactions, namely steam reforming [14] and oxo reforming [15].

$$CH_4 + H_2O \rightleftharpoons CO + 3\,H_2 \quad \text{steam reforming} \qquad [14]$$

$$CH_4 + 1/2\,O_2 \rightleftharpoons CO + 2\,H_2 \quad \text{oxo reforming} \qquad [15]$$

Figures 5 and 6 show the H_2/CO product ratio and the CH_4 and CO_2 conversion ($X(CH_4)$ and $X(CO_2)$) of a Rh(1%)/Al_2O_3 catalyst while consecutively replacing CO_2 by H_2O (Fig. 5) or O_2 (Fig. 6) at a reaction temperature of 750°C. All data are obtained at conditions far away from equilibrium. Even the fast WGS at this temperature was still far from equilibrium (20). No deactivation due to possible sintering or coking phenomena was observed irrespective of the H_2O or O_2 content in the feed gas. An increase in H_2/CO ratio always results from a reduction of CO_2 conversion, indicating that the reforming reactions of CH_4 with H_2O or O_2 are faster than the CH_4 reforming with CO_2.

By increasing the CO_2/CH_4 feed ratio the H_2/CO ratio can be lowered from 0.7 for a stoichiometric CO_2/CH_4 ratio of 1 : 1 to about 0.2 for a CO_2/CH_4 ratio of 5 : 1. In agreement with recent findings by Choudhary *et al.* (32), our results show that the H_2/CO ratios can be varied readily in a wide range ($0.2 < H_2/CO < 3$) and thus tailored to the technical needs of a process.

CONCLUSIONS

CO_2 reforming of methane under conditions of stoichiometric feed composition proceeds very effectively on Rh, Ru, and Ir catalysts. The activity of these catalysts can be correlated with the accessible metal surface area. Over a wide range of catalysts and supports studied, the rate per unit surface area (TOF) does not depend significantly on dispersion, indicating that CO_2 reforming at high temperatures is structure insensitive. No direct influence of the microstructure of the support on the reaction rates was detected. The influence of the support seems limited to the stabilization of the metal surface area, which in turn is responsible for catalyst activity. The present study, limited to reaction controlled conditions, shows that for the preparation of a highly active catalyst it is sufficient to consider one parameter, the accessible metal surface area. To optimize catalyst performance (high yield at low cost), the metal dispersion has to be maximized and has to be stable. This can be achieved by selected oxidation reduction pretreatments of the catalysts. Both γ-Al_2O_3 and the binary oxide ZrO_2(5%)/SiO_2 are especially good catalyst supports: Rh catalysts based on these supports not only showed high activity but also promise to be thermally stable even after long reaction times. Product composition can be easily controlled over a wide range of CO/H_2 ratios by partial substitution of CO_2 by H_2O or O_2 in the feed.

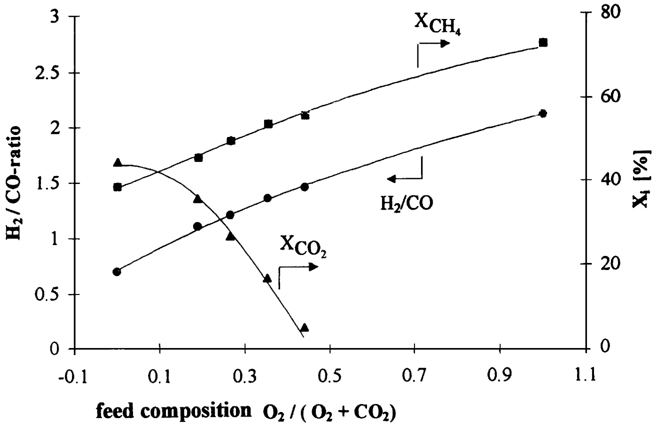

FIG. 6. Effect of oxygen addition to the feed on the product composition (reaction temperature 750°C. 1% Rh/γ-Al_2O_3, feed $\dot{n}_{CO_2,0} + \dot{n}_{O_2,0} = \dot{n}_{CH_4,0} = \text{const.}$).

REFERENCES

1. Ayers, W. M., (Ed.), “Catalytic Activation of Carbon Dioxide,” ACS Symposium Series 363. Am. Chem. Soc., Washington, DC, 1988.
2. Dibby, D. M., Chang, C., Howe, R. F., and Yurchak, S. (Eds.), “Studies in Surface Science and Catalysis,” Vol. 36. Elsevier, Amsterdam, 1988.
3. Fox III, J. M., *Catal. Rev.-Sci. Eng.* **35**, 169 (1993).
4. Rostrup-Nielsen, J.-R., and Bak-Hansen, J.-H., *J. Catal.* **38**, 144 (1993).
5. Erdöhelyi, A., Cserényi, J., Papp, E., and Solymosi, F., *Appl. Catal.* **108**, 205 (1994).
6. Ashcroft, A. T., Cheetham, A. K., Green, M. L. H., and Vernon, P. D. F., *Nature* **452**, 225 (1991).
7. Richardson, J. T., and Paripatyadar, S. A., *Appl. Catal.* **61**, 293 (1990).
8. Meirovitch, E., and Segal, A., *Sol. Energy* **46**, 219 (1991).
9. Gadalla, A., and Bower, B., *Chem. Eng. Sci.* **43**, 3049 (1988).
10. PC-program Equitherm 3.0, Verlag Chemie, Weinheim, 1994.
11. Bodrov, I. M., and Apel’baum, L. O., *Kinet. Catal.* **8**, 379 (1967).
12. Solymosi, F., Erdöhelyi, A., and Cserényi, J., *Catal. Lett.* **16**, (1992).
13. Zhang, Z. L., and Verykios, X. E., *Catal. Today* **21**, 589 (1994).
14. Swaan, H. M., Kroll, V. C. H., Martin, G. A., and Mirodatos, C., *Catal. Today* **21**, 571 (1994).
15. Tsipouriari, V. A., Efstathiou, A. M., Zhang, Z. L., and Verykios, X. E., *Catal. Today* **21**, 579 (1994).
16. Kurz, G., and Teuner, S., *Erdöl Kohle* **43**, 171 (1990).
17. Nakamura, J., Aikawa, K., Sato, K., and Uchijima, T., *Catal. Lett.* **25**, 265 (1994).
18. Erdöhelyi, A., Cserényi, J., and Solymosi, F., *J. Catal.* **141**, 287 (1993).
19. Mark, M. F., and Maier, W. F., *Angew. Chem. Int. Ed.* **33**, 1657 (1994).
20. Mark, M. F., Ph.D. Thesis, Universität Essen, 1995.
21. Mark, M. F., Mark, F., and Maier, W. F., to be published.
22. Brinker, C. F., and Scherrer, G. W., “Sol-Gel Science.” Academic Press, New York, 1990.

23. Maier, W. F., Tilgner, I.-C., Wiedorn, M., and Ko, H.-C., *Adv. Mater.* **5**, 726 (1993).
24. Ruckenstein, E., *in* "Metal-Support Interactions in Catalysis, Sintering and Redispersion" (S. A. Stevenson, J. A. Dumesic, R. T. K. Baker, and E. Ruckenstein, Eds.), Van Nostrand Reinhold Catalysis Series 141. Van Nostrand Reinhold, New York, 1987.
25. Jiang, X. Z., Hayden, T. F., and Dumesic, J. A., *J. Catal.* **83**, 168 (1983).
26. Smith, J. S., Thrower, P. A., and Vannice, M. A., *J. Catal.* **68**, 270 (1981).
27. Froment, G. F., and Bischoff, K. B., "Chemical Reactor Analysis and Design." Wiley, New York, 1979.
28. Bond, G. C., *Chem. Soc. Rev.* **20**, 441 (1991).
29. Fiedorow, R. M., and Wanke, S. E., *J. Catal.* **43**, 34 (1976).
30. Gates, B. C., "Catalytic Chemistry." Wiley, New York, 1992.
31. Maier, W. F., and Ko, H. C., *Catal. Today* **25**, 429 (1995).
32. Choudhary, V. R., Rajput, A. M., and Prabhakar, B., *Angew. Chem.* **106**, 2179 (1994).